Applied Energy 165 (2016) 612–626

Contents lists available at ScienceDirect

Applied Energy

journal homepage: www.elsevier.com/locate/apenergy

Experimental investigation of butanol isomer combustion in Homogeneous Charge Compression Ignition (HCCI) engines

J. Hunter Mack [a,*], Daniel Schuler [a,b], Ryan H. Butt [a], Robert W. Dibble [a]

[a] University of California at Berkeley, Berkeley, CA, United States
[b] Eidgenössische Technische Hochschule Zürich, Zürich, Switzerland

HIGHLIGHTS

- Isobutanol and n-butanol have a higher HCCI reactivity than gasoline.
- IMEPg is comparable for each fuel across all tested conditions.
- n-Butanol presented the highest ringing intensity at higher equivalence ratios.
- Gasoline exhibited the best combustion stability of all tested fuels.
- Emissions from n-butanol and isobutanol were similar across all tested conditions.

ARTICLE INFO

Article history:
Received 4 September 2015
Received in revised form 9 December 2015
Accepted 24 December 2015
Available online 7 January 2016

Keywords:
Homogeneous charge compression ignition
Internal combustion
Butanol
Experiments
Biofuel

ABSTRACT

Longer chain alcohols, such as butanol, possess major physiochemical advantages over ethanol as bio-components for gasoline, including higher energy content, better engine compatibility, and less water solubility. In this study, two butanol isomers (n-butanol and isobutanol) are investigated as potential fuels for Homogeneous Charge Compression Ignition (HCCI) engines. Wide ranges of intake pressure and equivalence ratio are investigated and the results are presented in comparison to ethanol and gasoline as reference fuels. Under all tested conditions, the butanol isomers require lower intake temperatures for a fixed combustion phasing, indicating higher HCCI reactivity. Both isomers show single-stage ignition behavior at all test points and behave similarly in regard to the combustion stability. Engine operation using n-butanol is slightly more stable under all conditions and misfiring occurs slightly later under very lean and naturally aspirated conditions. Similar to gasoline, n-butanol shows a higher heat release rate (HRR) at the beginning of combustion. The intermediate temperature heat release (ITHR) lowers the coefficient of variation (CoV) of IMEPg (gross indicated mean effective pressure), especially at retarded combustion timing and lean mixtures. However, the knock resistance of n-butanol is lower compared to isobutanol and the other tested fuels. The exhaust emissions of the two butanol isomers are in the same range as the two reference fuels. Overall, the results indicate that butanol is suited for use as a fuel in HCCI engines, either in neat form or in blend with gasoline.

1. Introduction

The increasing environmental impact of fossil energy sources, the limited availability of fossil fuels, and rising fuel prices have all contributed to an increased attention toward biofuel development. First-generation biofuels, such as ethanol produced from corn, have been used as a replacement for fossil fuels; however, concerns over feedstock competition with food sources and well-to-wheel CO_2 balances have precipitated the development of second-generation biofuels. Butanol, a potential alternative fuel, can be produced using a similar process to ethanol. Several studies have investigated butanol, typically as the isomer n-butanol, as a fuel in spark-ignited (SI) and diesel engines in both pure and blended forms [1–8]. However, the use of n-butanol in Homogeneous Charge Compression Ignition (HCCI) engines has only recently gained interest among the community [9–11]. HCCI, a low temperature combustion (LTC) strategy, offers high thermal efficiencies alongside low NOx emissions. The research objective of this study is to evaluate the HCCI combustion behavior of two

* Corresponding author at: University of Massachusetts Lowell, Lowell, MA, United States. Tel.: +1 978 934 5766.
E-mail address: hunter_mack@uml.edu (J.H. Mack).

http://dx.doi.org/10.1016/j.apenergy.2015.12.105
0306-2619/

Nomenclature

BDC	bottom dead center
CA50	crank angle at which 50% of the heat has been released
CAD	crank angle degree
CI	compression ignition
DME	dimethyl ether
EGR	exhaust gas recirculation
HCCI	homogeneous charge compression ignition
HCSI	homogeneous charge spark ignition
HRR	heat release rate
HTHR	high temperature heat release
IMEP	indicated mean effective pressure
ITHR	intermediate temperature heat release
LHV	lower heating value
LTC	low temperature combustion
LTHR	low temperature heat release
MON	motor octane number
NOx	oxides of nitrogen
PM	particulate matter
PRF	primary reference fuel
ROHR	rate of heat release
RON	research octane number
SI	spark ignition
TDC	top dead center
TDI	turbocharged direct injection
UHC	unburned hydrocarbons

butanol isomers, n-butanol and isobutanol, through a systematic experimental investigation.

1.1. Homogeneous charge compression ignition

Homogeneous Charge Compression Ignition (HCCI) has been extensively studied in the last decade. HCCI engines combine characteristics of both spark-ignited engines and diesel engines. These engines have a homogeneous mixture of fuel and air, similar to a spark-ignited engine, and compression-ignition like a diesel engine. The typical operating conditions of HCCI are at lean equivalence ratios (less than 0.4), thus the flame temperature is relatively low (usually well below 2000 K) and therefore NOx emissions are significantly lower compared to the traditional combustion methods [12]. The combustion process and the burn rate in HCCI are largely controlled by chemical kinetics. The temperature rise caused by the compression process is used to produce thermal conditions in which the fuel–air mixture autoignites.

There are several advantages of HCCI, including efficiencies similar to diesel engines. This improved efficiency has three sources: high compression ratios, elimination of throttling losses, and the shorter combustion duration [13]. Additionally, HCCI engines have lower engine-out NOx emissions relative to SI and diesel engines as a result of the relatively low combustion temperatures. HCCI engines also have much lower soot, or particular matter (PM), emissions in comparison to SI and diesel engines. The low PM emissions are primarily due to the lean dilute homogeneous air–fuel mixture, which allows for the absence of a diffusion flame and locally fuel-rich regions. Another advantage of HCCI combustion is its fuel-flexibility. HCCI operation has been shown using a wide range of fuels. The combustion of gasoline, diesel fuels, natural gas, and short chain alcohols has been studied in the past decade [14–18]. In this study, the performance of butanol isomers (isobutanol and n-butanol) is compared to that of gasoline and ethanol, two widely-used fuels in HCCI research.

There are also several challenges facing HCCI. Control of the autoignition event is one of the most difficult problems to solve, as HCCI ignition is largely controlled by the chemical kinetics and sensitive to intake temperature and in-cylinder composition. Furthermore, a change in engine speed has a dramatic effect on the amount of time for the autoignition chemistry to occur relative to the piston movement. Developing systems that compensate for these influencing factors, particularly for rapid transients, is an area of active research.

In HCCI engines, a large amount of the fuel/air mixture ignites simultaneously. Combustion can become very rapid and at higher loads and the richer fuel mixtures can lead to very high rates of heat and pressure rise. This results in high ringing intensities (high amplitude in-cylinder pressure fluctuations) that can damage the engine, lower operating efficiency, and unacceptable levels of NOx emissions. Due to this, HCCI engines tend to have a narrow operating range [19]. A combination of HCCI and SI operation is a possible solution to this problem, but it enlarges the complexity of the system. Poor cold start behavior, another challenge to HCCI, can also be solved by engine mode switching.

Another difficulty facing HCCI is the relatively high levels of UHC and CO emissions [20,21]. In general, there are two main formation routes of these emissions. First, a significant amount of air–fuel mixture is compressed and trapped in the crevice regions of the engine during the compression stroke [22]. In comparison to SI and CI engines, the exhaust gases in HCCI combustion present in the cylinder during the expansion stroke are relatively cold and thus the temperature is not sufficient to fully oxidize the gases coming out of the crevice regions. The second route of formation is due to a thermal boundary layer along the cylinder surfaces. Gases do not combust in these regions as a result of thermal quenching due to the relatively cooler in-cylinder surfaces [23].

1.2. Alternative fuels in HCCI engines

The use of biofuels in HCCI has been researched extensively over the last decade. A large variety of fuels have been investigated in regards to HCCI combustion and other LTC applications. This includes experimental studies using dimethyl ether (DME) in combination with methanol [24], multiple studies on ethanol [25–29], ethanol/iso-octane blends [16], isopentanol [30], and others.

In regards to butanol, early studies investigated the use of butanol in blended fuels. Butanol and n-heptane blends have shown higher indicated thermal efficiencies when compared to primary reference fuels (PRFs) [31]. Furthermore, the butanol blends had a later start of combustion and a slower rate of heat release compared to the PRF blends [31]. The impact of n-butanol and ethanol blending on the net heat release rate has also been quantified in comparison to PRFs. Higher ethanol, n-butanol, or iso-octane fractions reduced the low temperature heat release (LTHR) and increased the indicated mean effective pressure (IMEP) moderately [32]. The addition of both alcohols in n-heptane has more impact on delaying the HRR than that of iso-octane. It has also been found that increasing the butanol volume percentage in n-heptane blends delays the ignition timing while diminishing the characteristics of two-stage heat release [33]. The low temperature reactions were largely insensitive to equivalence ratio variations, but high temperature reactions were sensitive to a change in equivalence ratio. A recent study investigated isobutanol in a Reactivity Controlled

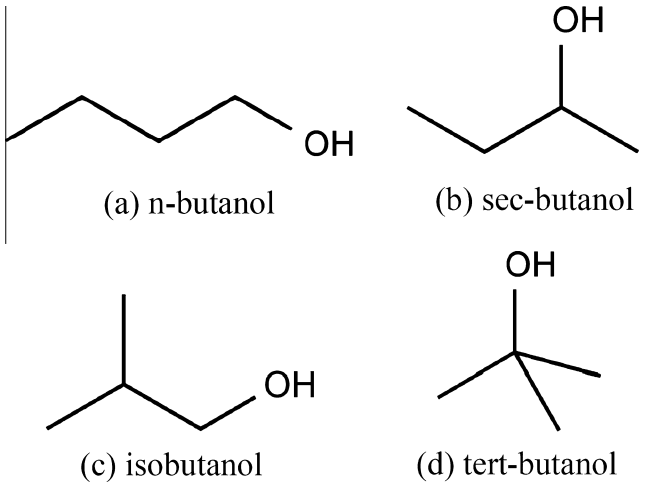

Fig. 1. Structure of the butanol isomers.

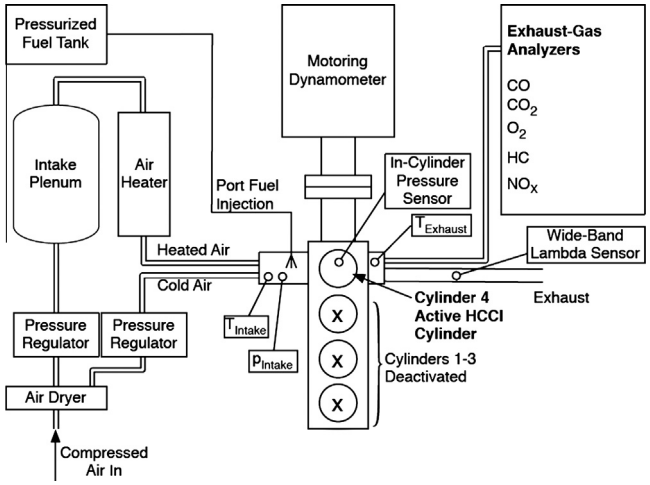

Fig. 2. Schematic of HCCI engine test bench, including intake system, and key diagnostic sensors.

Table 1
Properties of the butanol isomers, ethanol and gasoline [20,40,45].

Fuel	n-Butanol	Isobutanol	Ethanol	Gasoline
Lower heating value (LHV) (MJ/L)	26.9	26.6	21.4	30–33
Density (kg/m^3)	809.5	801.8	789.3	720–780
Research octane number (RON)	96	105	130	88–98
Motor octane number (MON)	78	94	96	80–88
Cetane number	25	–	8	0–10
Melting temperature (°C)	−89.5	−108	−114.1	–
Boiling temperature (°C)	117.7	108	78	35–200
Heat of vaporization (kJ/kg at 25 °C)	707.9	684.4	919.6	~351
Self ignition temperature (°C)	343	415.6	434	~300
Solubility in water at 20 °C (wt%)	7.7	8.7	Miscible	Negligible
Kinematic viscosity (cSt) at 20 °C	3.6	8.3	1.5	0.37–0.44

Table 2
List of engine specifications and operation conditions.

Configuration	4 cylinder
Displacement	1.9 L
Compression ratio	17.0: 1
Bore	79.5 mm
Stroke	95.5 mm
Connection rod length	144.0 mm
Fuel injection	Port fuel injection
Fuel pressure	45 PSI
Valves (intake, exhaust)	1, 1
Intake valve open (IVO)	2 °CA bTDC
Intake valve close (IVC)	47.5 °CA aBDC
Exhaust valve open (EVO)	47.5 °CA bBDC
Exhaust valve close (EVC)	8 °CA aTDC
Overlap	0 °CA
Maximum valve lift	10 mm
Engine speed	1800 RPM
Volume BDC	504.72 cm^3
Volume TDC	29.69 cm^3

Compression Ignition (RCCI) engine which features a secondary injection event in combination with a premixed charge of fuel and air, finding that isobutanol's large octane number required a significant secondary injection of a more reactive fuel (20% di-tert-butyl peroxide blended with isobutanol or diesel) to perform similarly to their baseline tests using gasoline as a primary fuel [34].

Butanol as a standalone fuel in HCCI engines has mainly been limited to studies using n-butanol. Engine performance, as measured by IMEP, was limited by combustion stability at lean conditions [10]. Ultra-low NOx and soot emissions were also achieved without the use of exhaust gas recirculation (EGR) at low- to mid-engine loads [9], while emissions were largely insensitive to intake pressure. The thermal efficiencies seen in the studies are comparable to that of conventional diesel combustion. The HCCI operating range of n-butanol is slightly smaller when compared to that of gasoline as a result of a lower IMEP [11]. To address this, the operating range of an n-butanol fueled HCCI engine was expanded using forced induction and residual gas trapping [35].

The increased interest in butanol as a fuel has also prompted several recent experiments on its chemical kinetics [36–38]. A recent experimental study showed similar rates of consumption for three butanol isomers, but significant differences in product formation and relative concentration [39]. The work presented here includes isobutanol, n-butanol, gasoline, and ethanol operated over a range of equivalence ratios, combustion timings, and intake pressures in a HCCI engine.

2. Materials and methods

2.1. Fuels

Butanol, and other longer chained alcohols, have significant advantages in terms of energy density, miscibility, and corrosivity in comparison with ethanol. Butanol has a four carbon structure and depending on the position of the hydroxyl (OH) group on the carbon chain, four different isomers are defined: n-butanol (1-butanol), sec-butanol, isobutanol (2-methyl-1-propanol), and tert-butanol. The structure of the four butanol isomers are shown in Fig. 1.

n-Butanol has a straight-chain structure with the alcohol at the terminal carbon. Sec-butanol is also a straight-chain molecule but the OH group is attached to an internal carbon. Isobutanol is a branched isomer with the OH group at the terminal carbon, while tert-butanol refers to the branched isomer with the OH group at an internal carbon.

Butanol, with the exception of tert-butanol, can be produced from sugars via fermentation or the catalytic conversion of synthesis gas (syngas) [20,40]. Tert-butanol does not exist in

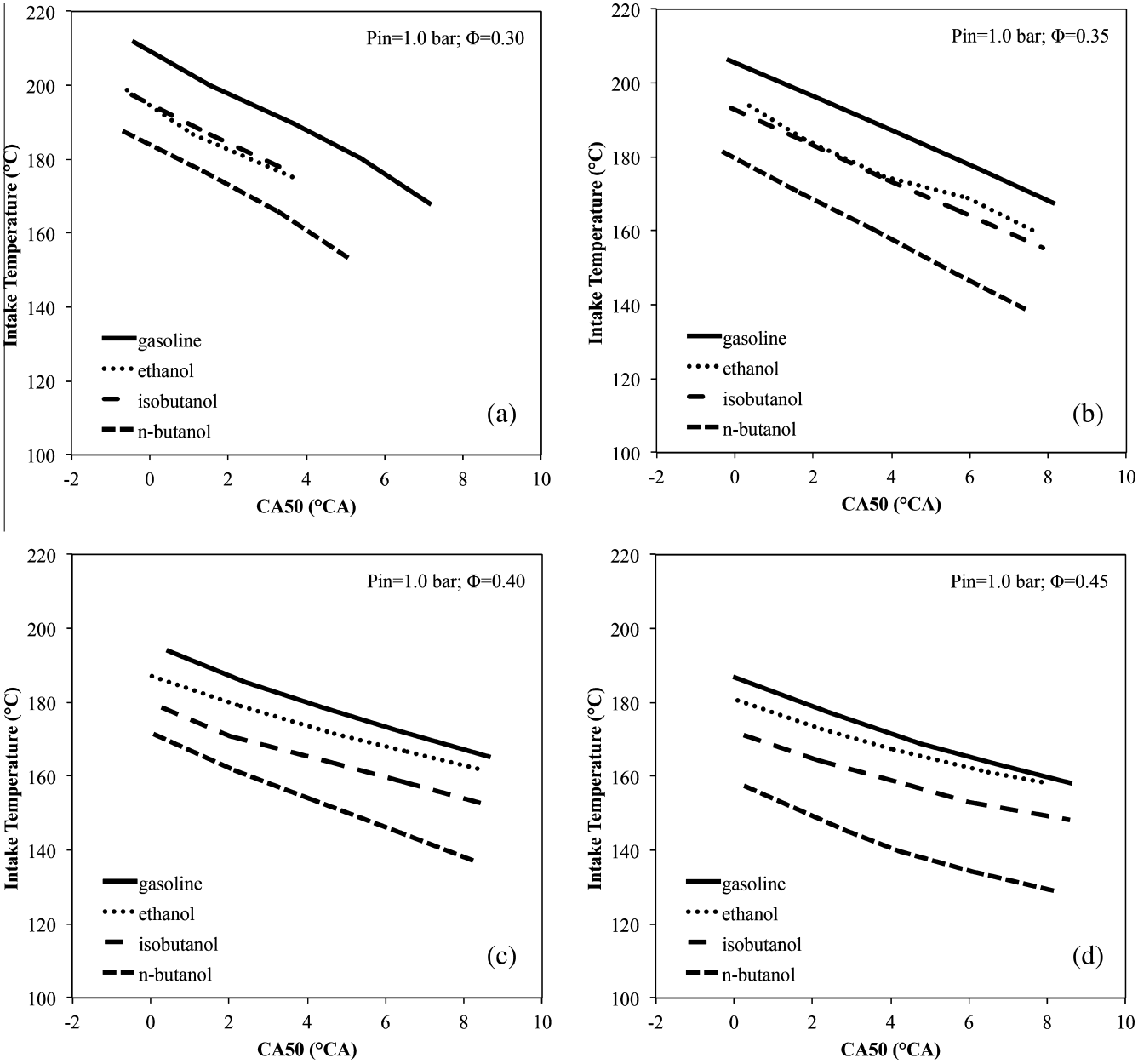

Fig. 3. Required intake temperature as a function of CA50 at different equivalence ratios (Φ) for gasoline, ethanol, n-butanol, and isobutanol; p_{intake} = 1.0 bar.

nature [41]. During the production of butanol from agricultural feedstock, n-butanol and isobutanol are heavily favored. Of all the isomers, n-butanol has been most widely studied as an engine fuel. The development of processes to generate isobutanol from biomass resources is an active research area, and its potential as a transportation fuel is gaining interest [42–44]. For these reasons, only two of the butanol isomers are experimentally investigated in this study: n-butanol and isobutanol. These butanol isomers are compared to ethanol and gasoline (commercial grade 91-octane gasoline sold in California, which includes up to 10% ethanol). The specific properties of the fuels under investigation are shown in Table 1. Standard gasoline contains a variety of hydrocarbons with different chain lengths; therefore, the fuel properties for standard gasoline are represented within a range of values rather than one specific number.

Butanol combines the advantages of gasoline in terms of energy density with the oxygen content and renewability of ethanol without being hydrophilic. The most important advantages of butanol over ethanol are:

- Butanol contains 25% more energy than ethanol on a volumetric basis.
- The heat of vaporization of butanol is less than half of that of ethanol, thus improving the cold start behavior of an engine running with butanol.
- The auto-ignition temperature of butanol (especially n-butanol) is lower than ethanol, which results in less ignition problems at low-load conditions and lower intake temperatures for a given combustion timing.
- Butanol is less corrosive than ethanol, improving compatibility with fuel systems.
- In blends with diesel or gasoline, butanol is less likely than ethanol to separate from the base fuel if the fuel is contaminated with water.

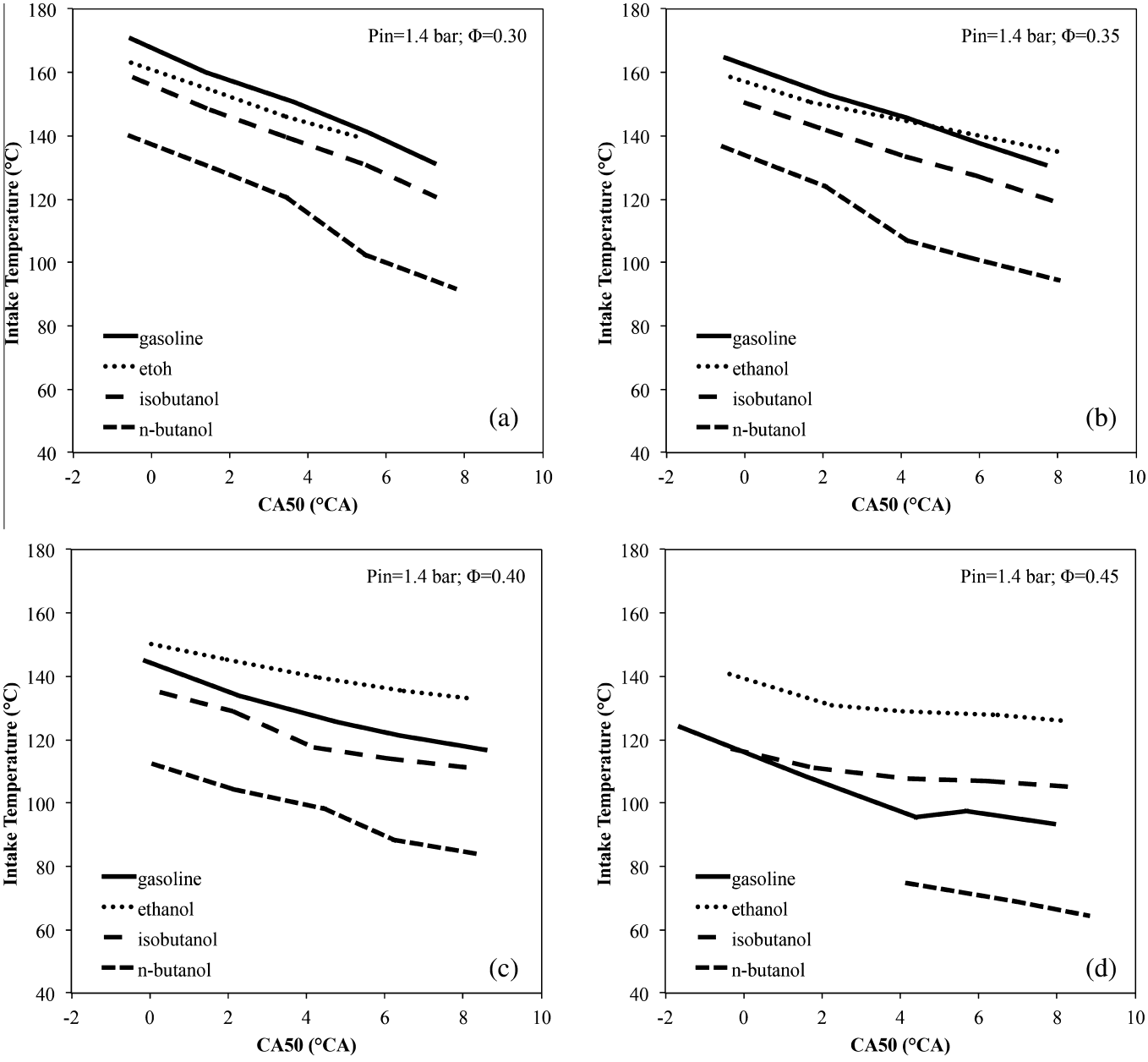

Fig. 4. Required intake temperature as a function of CA50 at different equivalence ratios (Φ) for gasoline, ethanol, n-butanol, and isobutanol; p_{intake} = 1.4 bar.

2.2. Experimental setup

The research engine used in the presented experiments is a modified four-cylinder 1.9 L Volkswagen TDI engine. The engine specifications and operating conditions are listed in Table 2.

The engine includes significant modification to enable operation in a HCCI mode:

- Replacement of the stock deep-bowl pistons with relatively flat pistons to reduce heat transfer.
- Modification of the glow plug holes to fit standard 10 mm spark plugs, which serve as the ion sensors.
- Insertion of in-cylinder quartz piezoelectric pressure transducers (AVL QH33D) into the direct fuel injector ports.
- A custom intake manifold including a port fuel injector system.
- A custom injection control system using solid-state relays and control signals generated from a National Instruments Labview program.
- Wide-band lambda sensors installed in the exhaust manifolds to monitor equivalence ratio.
- Isolation of the exhaust manifold from cylinder 4 to ensure accurate measurement of the equivalence ratio.
- Replacing the stock turbocharger with an external 100 HP compressor (and a 6 m^3 surge tank) to achieve boosted intake conditions.
- A Kulite XTEL 190(M) piezoresistive pressure sensor to measure the intake pressure near the intake valve at a crank-angle resolution.
- Temperature measurement in the intake and exhaust system using multiple K-Type thermocouples.

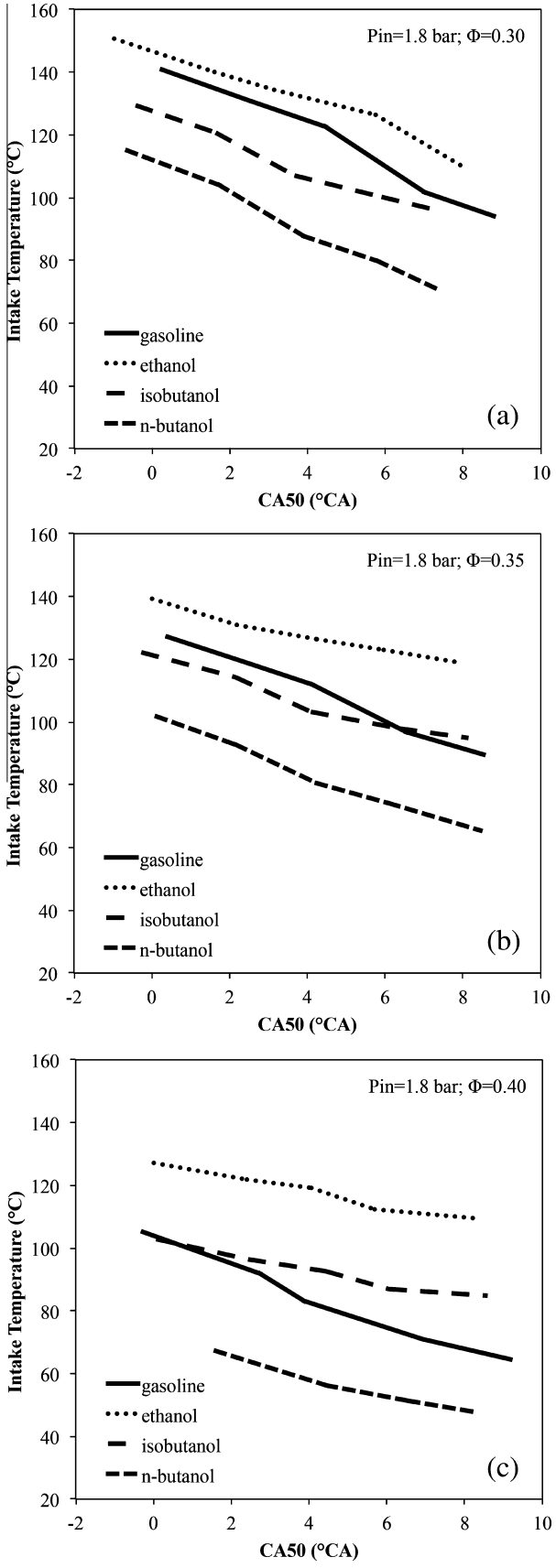

Fig. 5. Required intake temperature as a function of CA50 at different equivalence ratios (Φ) for gasoline, ethanol, n-butanol, and isobutanol; p_{intake} = 1.8 bar.

Engine speed is controlled with an AC motor-generator connected to the engine using a direct-drive shaft and clutch. For this study, the motor-generator does not include a variable frequency drive and therefore the engine speed is maintained at 1800RPM regardless of whether the engine is firing or motoring. Fig. 2 shows a schematic of the HCCI engine test bench and key sensors for the data acquisition and control. The engine has been converted for single-cylinder operation by deactivating cylinders 1–3 and the configuration of the engine facility and data acquisition is similar to previous studies [46,47].

Each cylinder includes an in-cylinder pressure transducer connected with a charge amplifier. The pressure measurements are triggered by a crankshaft encoder with a resolution of 4 samples per degree crank angle. At each test point, 300 consecutive thermodynamic cycles are measured and recorded. The pressure data is used to calculate heat release, indicated mean effective pressure, and indicated efficiency. The most important recorded parameters for the controlling of the engine and the evaluation are: intake pressure (p_{intake}), intake temperature (T_{intake}), in-cylinder pressure ($p_{incylinder}$), equivalence ratio (Φ), exhaust temperature ($T_{exhaust}$), coolant temperature ($T_{coolant}$), and oil temperature (T_{oil}). During engine operation the coolant and oil temperatures are kept in a constant range to guarantee comparable results.

The CA50, calculated from the in-cylinder pressure data, is monitored in real-time while testing and serves as a feedback parameter for the intake temperature T_{intake}, which is controlled by adjusting the intake air heater. As the intake temperature is increased, combustion timing is advanced. As shown in Fig. 2, the intake temperature is fine-tuned by adjusting the amount of mass flow of hot air and cold (ambient temperature) air. The amount of cold air is regulated via the pressure regulator installed upstream of the intake in the cold air supply.

Fuel is port injected in the intake manifold of cylinder 4 after the mixing of hot and cold air. The fuel injector is connected to a 12 V battery through a solid-state relay, which allows control of the amount of fuel injected by varying the pulse width. The equivalence ratio is measured using wideband lambda sensors (Innovate Motorsports LC-1) installed in the exhaust manifold of cylinder 4. These lambda sensors generate an analog voltage output that is proportional to the oxygen or unburned fuel fraction in the exhaust. The value given out by the lambda sensor is used to control the pulse width of the fuel injection by a feedback control loop.

The experimental procedure consisted of setting a desired intake pressure and equivalence ratio for a given fuel. The intake temperature was then modulated to acquire the desired combustion timing (CA50). This process was repeated for each fuel after allowing for sufficient time to flush any residual fuel from the injection system.

2.3. Data acquisition and post-processing

The data was collected at stable, non-transient engine operating points with constant intake conditions (temperature, pressure, and equivalence ratio). Each test point was replicated for consistency in the results.

The experimental data was post-processed to calculate the rate of heat release (ROHR) and the in-cylinder temperature profiles. The process used in this study was the same as used in previous studies [47]. A Savitzky–Golay filter with 19 points [48] is used in conjunction with three hundred consecutive cycles for each average pressure trace. The average pressure traces serve as basis for post-processing. The ROHR model included blow by and wall heat losses, defined using a Woschni model and using calibration factors determined from cycle simulation calculations [49]. The

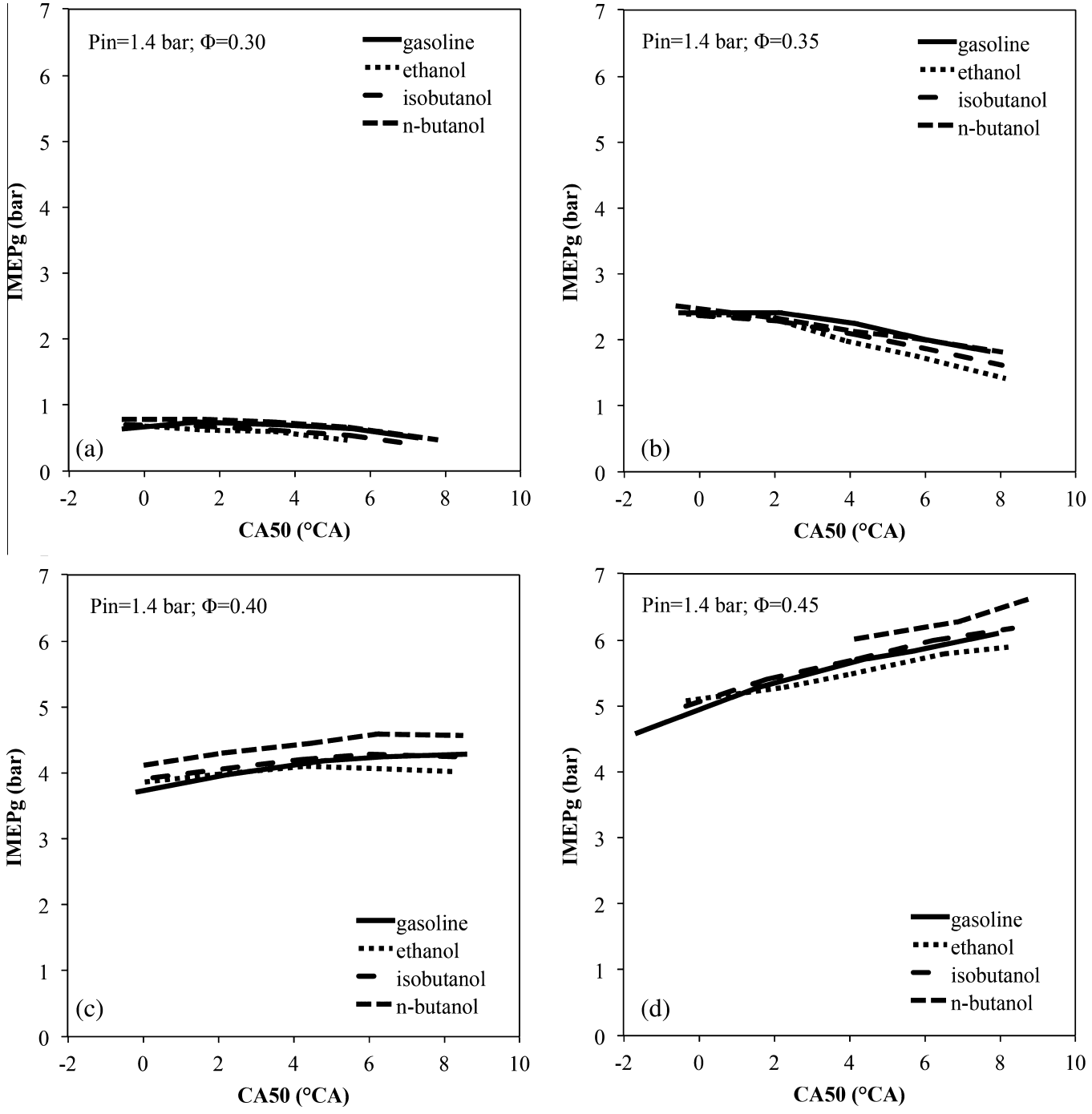

Fig. 6. Power output (gross IMEP) as a function of CA50 at different equivalence ratios (Φ) for gasoline, ethanol, n-butanol, and isobutanol; p_{intake} = 1.4 bar.

thermodynamic properties of the mixture are calculated by using Lawrence Livermore National Laboratory (LLNL) and National Aeronautics and Space Administration (NASA) polynomials of the species included in the mixture. It is assumed that the mixture during the compression stroke consists of fuel, air, and residual gases. The amount of residual gas is determined by a cycle simulation calculation. The composition of the residual gas after combustion is defined by the combustion products assuming complete combustion. During combustion, the change from initial mixture to combustion products is assumed proportional to the Vibe combustion profile with an assumed start and end of combustion determined by an iterative process [50]. After the ROHR is calculated, the new start and end of combustion is calculated and compared with the assumed values. If the difference between the start and end values are within a defined tolerance, the iteration is completed. In-cylinder temperature is calculated by using the ideal gas equation and calculated profiles of mass, volume, and composition during the closed portion of the cycle.

Ringing intensity is calculated by using Eq. (1) where $(dp/dt)_{max}$ is the maximum pressure rise rate, p_{max} is the peak in-cylinder pressure, T_{max} is the maximum of mass averaged in-cylinder temperature (calculated with the ideal gas law), γ is the ratio of specific heats (c_p/c_v), R is the universal gas constant, and β is a tuning parameter which relates the amplitude of pressure pulsations with the maximum pressure rise rate [51]. The tuning parameter β is set to 0.05 in this analysis. A common ringing intensity limit is 5 MW/m^2 based on the onset of audible knocking and the appearance of pressure pulsations [48].

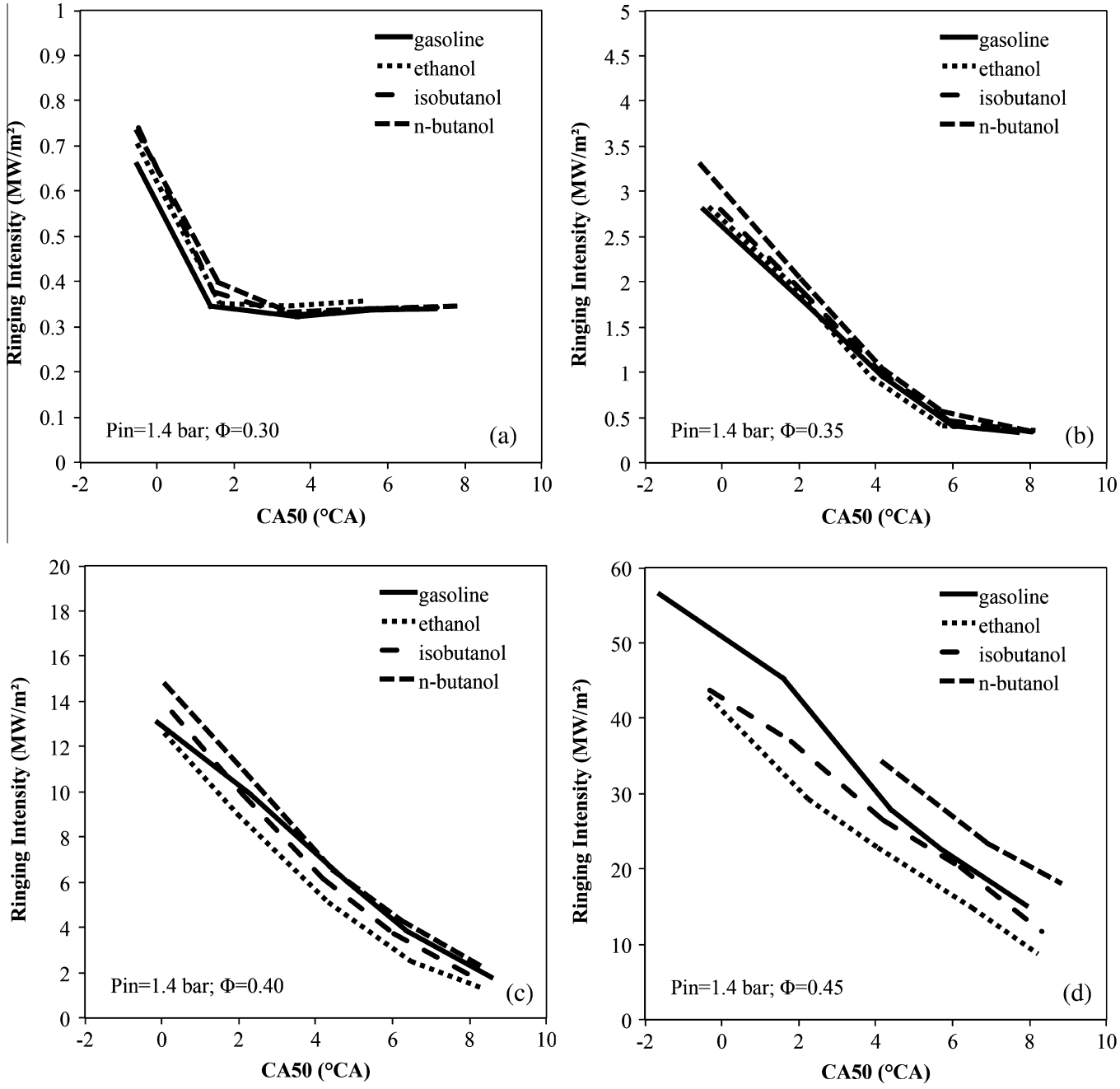

Fig. 7. Ringing intensity as a function of CA50 at different equivalence ratios (Φ) for gasoline, ethanol, n-butanol, and isobutanol at an intake pressure of 1.4 bar. Note the different scales in the vertical axis.

$$\text{Ringing intensity} \approx \frac{1}{2\gamma} \cdot \frac{\beta\left(\frac{dp}{dt}\right)_{max}}{p_{max}} \cdot \sqrt{\gamma R T_{max}} \quad (1)$$

The coefficient of variation (CoV) of IMEPg is generally used to compare the combustion stability. It has been found that vehicle drivability problems can occur when CoV IMEPg exceeds about 10% [52]. CoV IMEPg is defined as the standard deviation of IMEPg (σ_{IMEPg}) divided by the mean IMEPg, as shown in Eq. (2).

$$\text{CoV IMEPg} = \frac{\sigma_{IMEPg}}{\text{IMEGg}} \cdot 100 \quad (2)$$

Water is condensed out of the sampled exhaust stream before reaching the gas analyzer, and thus the results should be interpreted as dry concentrations. Exhaust emissions are continuously sampled from the exhaust manifold attached to cylinder 4, located directly before the exhaust manifold converges into a common stream. The Horiba gas analyzer includes separate analyzers to determine concentrations of unburned hydrocarbons (flame ionization), oxygen (magneto-pneumatic), carbon monoxide (infrared), carbon dioxide (infrared), and nitric oxides (chemiluminescent). Emissions values were used in post-processing to validate the measured equivalence ratios.

2.4. Experimental uncertainty

The in-cylinder pressure signal is averaged over 300 consecutive cycles with a cycle-to-cycle variation of <1%. Combustion timing, as defined by CA50, varied by <0.25° for all test conditions. Small variations in emissions data (6% for NOx, <2% for other emissions) were observed. The low NOx emissions are near the threshold of

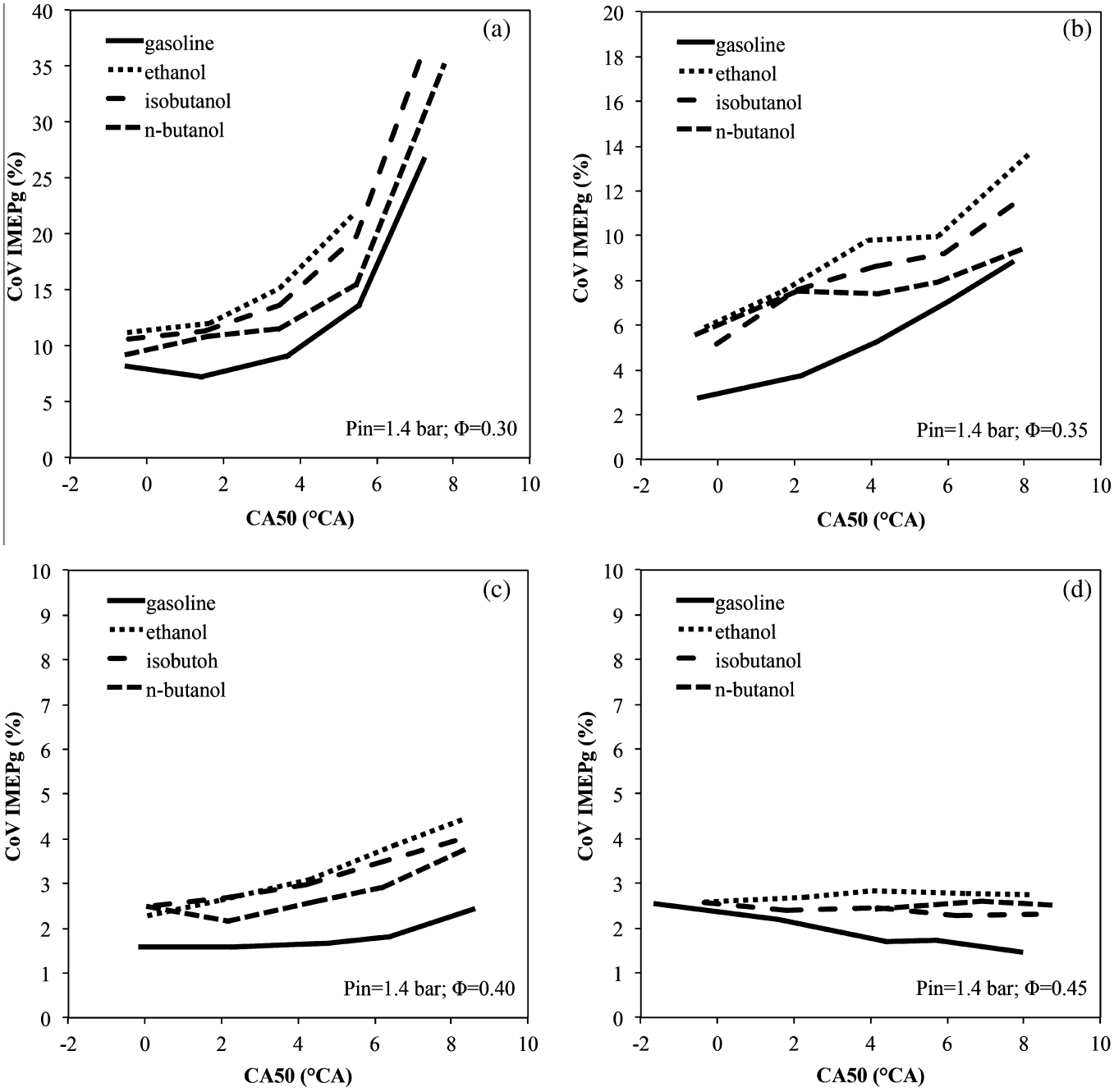

Fig. 8. IMEPg coefficient of variation as a function of CA50 at different equivalence ratios Φ for gasoline, ethanol, n-butanol, and isobutanol at an intake pressure of 1.4 bar. Note the different scaling used for the vertical axis.

the analyzer, which accounts for the variability in those measurements. Since the error in the measurements is small, error bars have been omitted from the presented results for the sake of clarity.

3. Results and discussion

Experiments were conducted at a variety of intake pressures (1.0, 1.4, and 1.8 bar), equivalence ratios (0.3, 0.35, 0.40, and 0.45), and CA50 (0, 2, 4, 6, and 8 °aTDC) for the following fuels: n-butanol, isobutanol, gasoline, and ethanol. In some tests, operating conditions were limited by misfire (lean Φ, late CA50) or excessive ringing (high intake pressure, early CA50) and thus are not included in the analysis. In an effort to reduce redundancy, a single intake pressure (1.4 bar) is presented rather than all 3 cases when the trends are the same and the additional plots are not additive to the discussion. Maximum values relevant to the analysis and discussion are presented for appropriate conditions.

3.1. Fuel reactivity and intake temperature sensitivity

The overall reactivity in HCCI combustion can be characterized in regard to the combustion phasing under defined engine operating conditions. More reactive fuels have more advanced combustion phasing than less reactive fuels. Alternatively, combustion phasing can be held constant for different fuels while the operation conditions are varied to investigate the differences in fuel reactivity. The required intake temperature for a given CA50 is an important parameter. Reactive fuels require lower intake temperatures

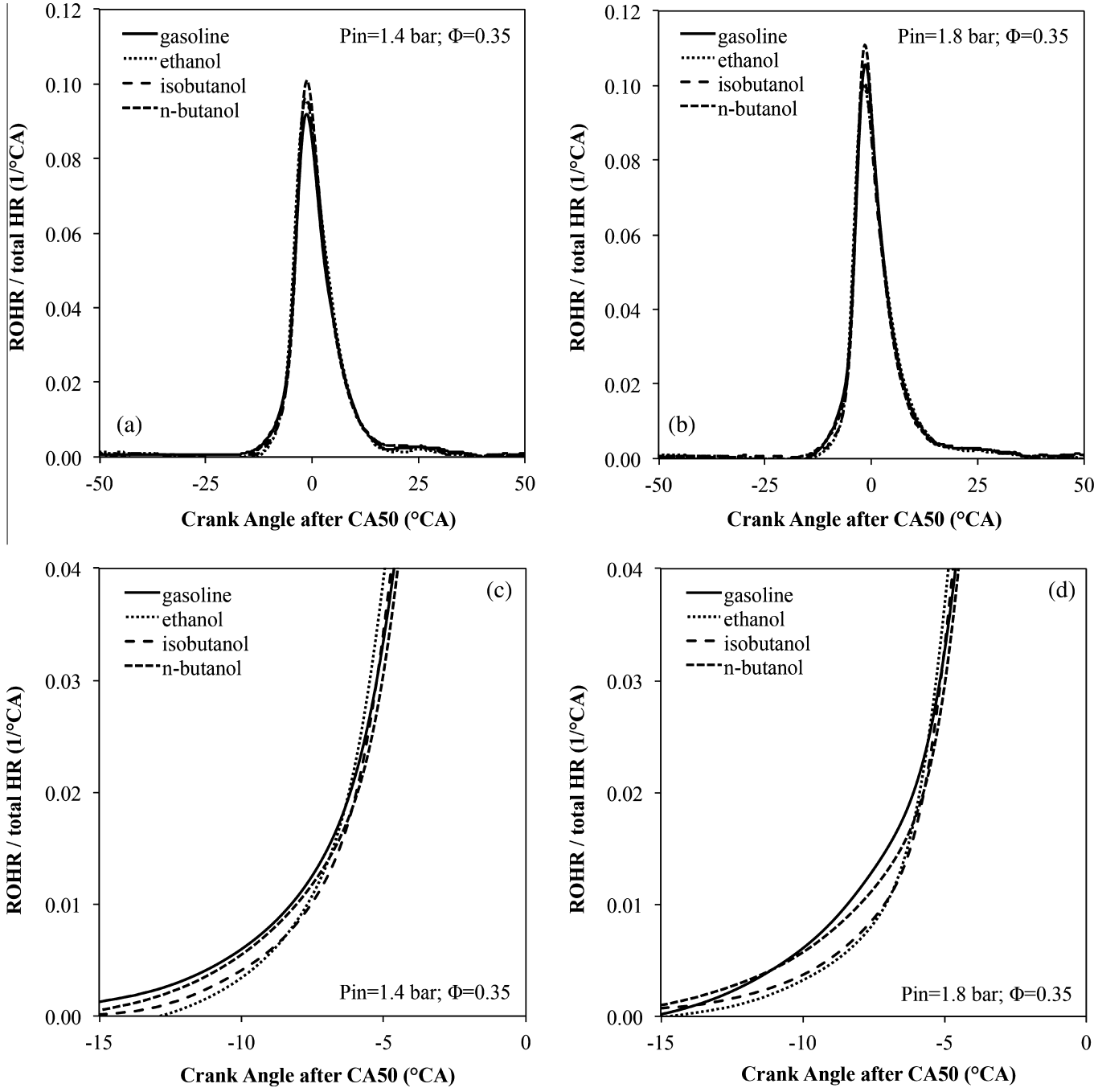

Fig. 9. Heat release rates at constant intake pressure (a and c – 1.4 bar; b and d – 1.8 bar), equivalence ratio (Φ = 0.35), and combustion phasing (approximately 8 CA aTDC). The traces have all been aligned so that CA 50 occurs at 0 CAD on the *x*-axis. The unaligned CA50's deviated by ±1.0 CAD.

for a given combustion phasing compared to a less reactive fuel. Additionally, the influence of higher intake pressures, or boosted conditions, on fuel reactivity is also important in regards to HCCI operation.

Fig. 3 shows the required intake temperatures (T_{intake}) to achieve the desired CA50 values for the 4 fuels at a fixed engine speed of 1800 RPM and an intake pressure of 1.0 bar. Each subplot of Fig. 3 includes a different equivalence ratio. All four fuels exhibit single-stage ignition behavior with almost no low temperature heat release (LTHR). As a result, the intake temperatures are in the same range and comparable. The degree of response of combustion phasing to a change of T_{intake} will be referred to as T_{intake} sensitivity.

With increasing equivalence ratio (Φ), as well as with increasing intake pressure (p_{intake}), the required intake temperature decreases for all 4 fuels. The difference between the intake temperatures of the different fuels increases with rising Φ. Under all conditions, n-butanol has the lowest required intake temperatures and thus is the most reactive fuel for HCCI operation in these experiments. The butanol isomers (isobutanol and n-butanol) behaved quite differently across all combustion timings and equivalence ratios. At lower Φ, the reactivity of isobutanol was found to be comparable with ethanol; as the equivalence ratio is increased, isobutanol shows a greater increase in reactivity than ethanol.

As the intake pressure is increased, the required intake temperature for a given CA50 of n-butanol decreases when compared to

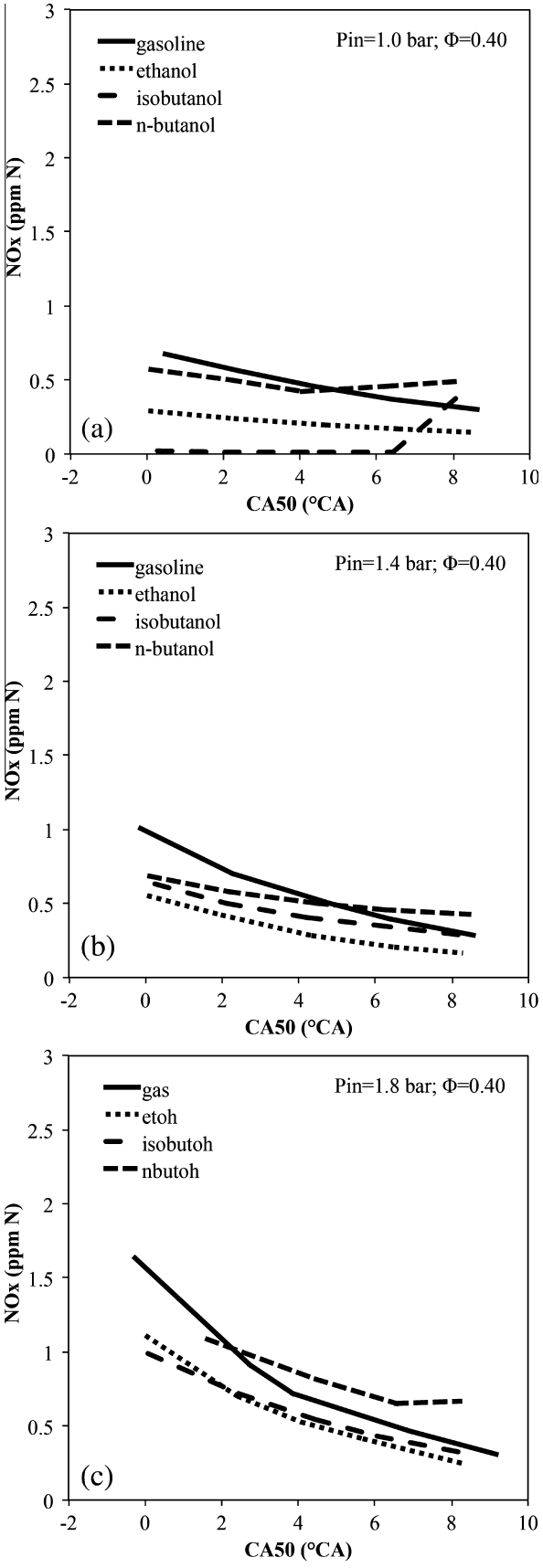

Fig. 10. NOx emissions as a function of CA50 at different intake pressures for gasoline, ethanol, n-butanol, and isobutanol; $\Phi = 0.40$.

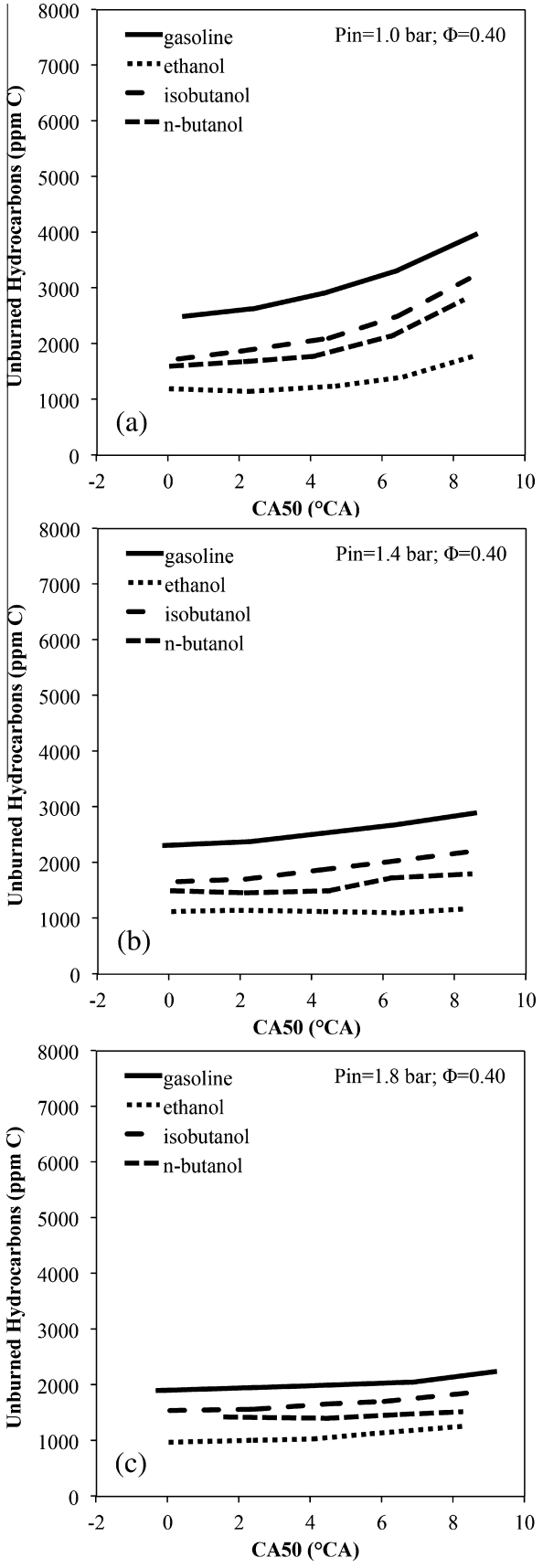

Fig. 11. UHC emissions as a function of CA50 at different intake pressures for gasoline, ethanol, n-butanol, and isobutanol; $\Phi = 0.40$.

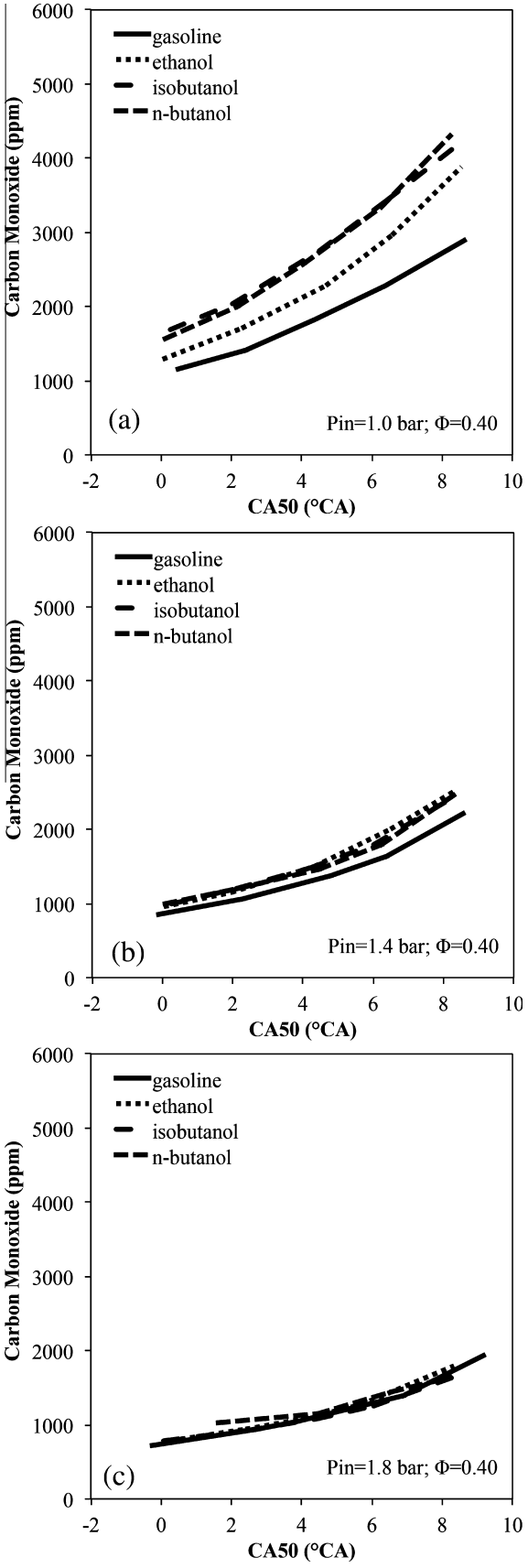

Fig. 12. CO emissions as a function of CA50 at different intake pressures for gasoline, ethanol, n-butanol, and isobutanol; $\Phi = 0.40$.

isobutanol. This suggests that n-butanol has a greater pressure sensitivity than isobutanol. Ethanol is the least pressure sensitive of the fuels and the required intake temperature decrease is relatively more gradual when compared to the other fuels. Figs. 4 and 5 show the required intake temperature as a function of CA50 for each fuel at 1.4 bar and 1.8 bar, respectively. At boosted conditions of $p_{intake} = 1.8$ bar, engine operation is limited to $\Phi \leqslant 0.4$ bar due to excessive ringing at the higher equivalence ratios.

In addition to different intake temperature requirements for each fuel, the slopes of the plots in Figs. 3–5 are also varied. The slope seen for ethanol is slightly less steep than the other three fuels under all investigated conditions. The n-butanol trends are almost parallel to the gasoline trends over the different combustion timings, indicating a comparable sensitivity to changes in equivalence ratio and intake pressure. Isobutanol behaves more similar to ethanol in the tests, rather than its isomer n-butanol.

Overall, the relative fuel reactivity and intake temperature sensitivity for the two butanol isomers is in agreement with the results presented in numerous kinetic modeling studies [36–38], as outlined in the introduction. Isobutanol consistently requires a higher intake temperature than n-butanol, which is consistent with the behavior found in the literature.

3.2. Indicated mean effective pressure (IMEP)

Fig. 6 shows the power output (as defined by gross indicated mean effective pressure, IMEGg) for different equivalence ratios and combustion timings at an intake pressure of 1.4 bar. Gross IMEP is used instead of net IMEP because these experiments used an external compressor for providing the boost pressure without adding exhaust backpressure from a turbocharger, allowing for separation of the effects of boost pressure.

The curves in Fig. 6 show that the power output rises with increased equivalence ratios for all fuels. The same trends were seen at intake pressures of 1.0 and 1.8 bar. The maximum IMEPg (7.2 bar) occurred using n-butanol at an intake pressure of 1.8 bar and a CA50 of 8 °aTDC. The test points for the lower equivalence ratios also show a decreasing IMEP as the combustion timing is retarded, caused in large part by lower peak in-cylinder pressures and lower combustion efficiencies at delayed combustion timings. This trend is reversed for the higher equivalence ratios (0.40 and 0.45) due to increased combustion stability at later CA50 values.

For the higher Φ conditions, a lower power output is observed at highly advanced combustion timing (near TDC). This effect is primarily due to three factors: (1) increased heat loss from higher peak temperatures that are achieved at advanced combustion timings, (2) increased time for heat transfer to occur, and (3) the early pressure rise from the autoignition process for highly advanced combustion timing causes some work against the piston before reaching TDC.

Ethanol had the lowest IMEPg at all tested conditions, as expected due to its significantly lower LHV (see Table 1). The power output from n-butanol, and isobutanol to a lesser extent, is comparable to gasoline. The lower intake temperatures at each CA50 when compared to gasoline are advantageous to the power output, overcoming the lower LHV values of the butanol isomers.

3.3. Ringing intensity

Fig. 7 shows the ringing intensities of the four fuels at different equivalence ratios at an intake pressure of 1.4 bar. At and below equivalence ratios of 0.35 allow for operation within the acceptable

ringing limit for all tested combustion timings. As Φ is increased, combustion timing has to be retarded to meet the given limit. At $\Phi = 0.45$ under boosted conditions, the ringing intensity for all test points is above the limit. It is worth noting that the highest IMEGg for $p_{intake} = 1.4$ bar occurs at late CA50, which corresponds to an acceptable ringing limit even at the elevated intake pressure and high Φ. This suggests that slightly delayed combustion timing can allow for stable combustion, higher power output, and acceptable ringing intensity performance.

These increases in ringing intensity can be explained in terms of the peak pressure rise rate, which constitutes a squared term in Eq. (1). Ringing increases with higher equivalence ratios and higher intake pressures because more energy is released as increased amounts of fuel and air are provided to the engine. For higher intake pressures, more fuel is injected to meet the desired equivalence ratio. Additionally, the rate of energy release (and thus the rate of pressure rise) in an almost uniform autoignition event is greater for higher equivalence ratios. Ringing increases with advanced combustion timing because the rate of piston expansion counteracting the pressure rise from autoignition is lower at advanced combustion timings.

For higher intake pressures, n-butanol is more likely to ring in comparison to the other fuels. n-Butanol has larger sensitivity to intake pressure in comparison to the other fuels. At $p_{intake} = 1.8$ bar and $\Phi = 0.45$, early combustion timings of CA50 < 4 °CA were unachievable due to tremendous ringing. The autoignition event is faster for a highly reactive fuel like n-butanol, which leads to a higher pressure rise rate and subsequently a higher ringing intensity.

The ringing intensity behavior of isobutanol is similar to ethanol at all intake pressures. These two fuels exhibit comparably high RON and MON values and therefore are more knock resistant. The autoignition event is slower and the ringing intensity under most conditions is slightly lower than that of gasoline and n-butanol.

3.4. Combustion stability

Stable combustion, with low cycle-to-cycle variations, is important to HCCI engine operation, especially at late combustion timings. All tested fuels experienced an increase in cycle-to-cycle variations as CA50 is retarded. This is partially explained due to an increased expansion rate at late CA50, which produces an increase in charge cooling. This counteracts the temperature rise associated with early exothermic reactions. In addition to larger CoV IMEP, delayed combustion timings also decrease the pressure rise rate and excessive delays can result in misfire. Fig. 8 shows CoV IMEPg for an intake pressure of 1.4 bar, with each subplot containing a different equivalence ratio. The presence of significant misfire events, and thus a high CoV IMEP, can clearly be seen in Fig. 8a at a CA50 of 8 °aTDC and an equivalence ratio of 0.3.

The two butanol isomers behave similarly in regard to the combustion stability, where n-butanol seems slightly more stable under all conditions and a later occurrence of misfire. Ethanol's CoV IMEPg is the largest across all operating conditions, while gasoline's is the lowest. Pure fuels methane, ethanol, and n-butanol have been shown to have a larger CoV IMEPg than gasoline, due in part to gasoline's multi-component constituency [53]. Lower equivalence ratios present a higher CoV IMEPg for all fuels and an increased tendency toward misfire at later combustion timings. These trends are also evident at intake pressures of 1.0 and 1.8 bar.

3.5. Heat release

Intermediate temperature heat release (ITHR), which occurs prior the high temperature heat release (HTHR), plays an important role in the combustion stability [54]. As combustion timing retards beyond TDC, the ITHR helps to maintain a high in-cylinder temperature that compensates for the declining cylinder temperature caused by piston expansion. At the operating conditions used in these experiments, all of the fuels present a single-stage heat release, without the presence of low temperature heat release (LTHR).

Fig. 9 shows the rate of heat release (ROHR) for all four fuels at fixed intake pressures (Fig. 9a and c at 1.4 bar; Fig. 9b and d at 1.8 bar) and equivalence ratio ($\Phi = 0.35$). The combustion timing is aligned at 8 °aTDC. The values have been normalized to the total heat release to provide better comparison between the fuels. The *x*-axis of lower subplots (Fig. 9c and d) is re-scaled to emphasize the differences in ITHR between the fuels.

Gasoline and n-butanol show a higher heat release rate at the beginning of combustion, which correlates to the lower CoV IMEPg values seen in Fig. 8. The appearance of ITHR lowers the CoV IMEPg of the engine, especially at retarded combustion timing and lean mixtures. This effect is slightly reduced at higher equivalence ratios. Delayed combustion timing using fuels with higher ITHR allows for improved HCCI performance due to less heat loss, a lower ringing intensity, and the ability to achieve a high power output.

3.6. Emissions

Oxides of nitrogen (NOx) emissions for different test conditions are shown in Fig. 10 for a given equivalence ratio ($\Phi = 0.40$) and intake pressures of 1.0, 1.4, and 1.8 bar. The results show the expectedly low NOx emission (<5 ppm) for HCCI over all experiments. Net NOx emissions generally increase with advanced combustion timings, higher equivalence ratios, and higher intake pressure. These results are not normalized to power output, and direct comparison between the values is difficult as measurement error (±1 ppm) is large in comparison to the reported values. The trends for NOx emissions can be partially explained in terms of peak in-cylinder temperatures. NOx formation mechanisms are highly temperature dependent, and in-cylinder temperatures are higher at advanced combustion timing and higher equivalence ratios. All four fuels considered in this study behave similarly.

Figs. 11 and 12 respectively show the unburned hydrocarbon (UHC) and carbon monoxide (CO) emissions for the same test conditions as Fig. 10. The trends from the two figures show that the hydrocarbon and carbon monoxide emissions increase with delayed combustion timing. Unburned hydrocarbon emissions and CO emissions generally increase with delays in combustion timing due to a decrease in in-cylinder temperatures, which inhibit complete oxidation. Additionally, CO and UHC emissions decrease with an increase in intake pressure. This is again explained by the role of in-cylinder temperature on oxidation reactions.

Higher equivalence ratios also lead to lower CO and UHC emissions, as explained by the diminished combustion efficiency at low equivalence ratios. Peak in-cylinder temperatures are the lowest at small Φ and delayed combustion timing, resulting in the largest relative CO and UHC emissions. The differences in CO and UHC emissions between the butanol isomers are quite small and within the measurement accuracy of the sampling device, especially at higher intake pressures. Gasoline has slightly higher UHC emissions over all tested conditions in comparison to the butanol isomers, while the lowest UHC emissions are achieved by ethanol. Gasoline had the lowest CO emissions and the butanol isomers presented similar emissions behavior across all tested conditions.

4. Conclusions

Two butanol isomers, n-butanol and isobutanol, were investigated as potential biofuels for Homogeneous Charge Compression

Ignition (HCCI) engines. Experiments were conducted on an automotive-scale HCCI engine in single-cylinder mode at a wide range of intake pressures, equivalence ratios, and combustion timings. In addition to n-butanol and isobutanol, gasoline and ethanol were tested as a means of comparison. N-butanol and isobutanol performed adequately as HCCI fuels and each maintained single-stage ignition characteristics for all tested operation points. The HCCI reactivity of n-butanol and isobutanol are higher than that of gasoline, as indicated by lower intake temperature requirements at constant combustion timings. Power output, presented as gross IMEP, is comparable for all four fuels across all conditions, though n-butanol presented the highest IMEPg values. While the two butanol isomers behave quite similar in regard to the combustion stability, n-butanol was slightly more stable under all conditions and misfire occured later under very lean and naturally aspirated conditions. However, the knock resistance of n-butanol is lower compared to isobutanol and the other tested fuels. The emissions produced by combustion of the two butanol isomers are very similar to those of gasoline and ethanol, with NOx emissions expectedly low due to HCCI operation. Overall, this study shows that in addition to their superior physiochemical properties compared to ethanol, n-butanol and isobutanol have similar HCCI combustion properties to gasoline. The butanol isomers, each with distinct advantages, appear to be a better choice as a gasoline-blending agent compared to ethanol in regard to their HCCI combustion properties.

Acknowledgements

This study was supported by LLNL under award number B586434 (Low Temperature Combustion Chemistry at Boost Pressures for Surrogate Fuels and Ethanol Use in HCCI Engine Experiments). Daniel Schuler would like to acknowledge Prof. Konstantinos Boulouchos of the Aerothermochemistry and Combustion Systems Laboratory at ETH Zürich for his support. The authors would also like to thank Darko Kozarac and David Vuilleumier for their contributions to the engine experiments and analysis.

References

[1] Wallner T, Miers SA, McConnell S. A comparison of ethanol and butanol as oxygenates using a direct-injection, spark-ignition engine. J Eng Gas Turb Power 2009;131(3).
[2] Ashraf E. Experimental study on emissions and performance of an internal combustion engine fueled with gasoline and gasoline/n-butanol blends. Energy Convers Manage 2014;88:277–83.
[3] Szwaja S, Naber JD. Combustion of n-butanol in a spark-ignition IC engine. Fuel 2010;89:1573–82.
[4] Gu X, Huang Z, Ca J, Gong J, Wu X, Lee C-f. Emission characteristics of a spark ignition engine fuelled with gasoline-n-butanol blends in combination with EGR. Fuel 2012;93:611–7.
[5] Broustail G, Halter F, Seers P, Moréac G, Mounaim-Rousselle C. Comparison of regulated and non-regulated pollutants with iso-octane/butanol and isooctane/ethanol blends in a port-fuel injection spark-ignition engine. Fuel 2012;94:251–61.
[6] Armas O, García-Contreras R, Ramos Á. Pollutant emissions from engine starting with ethanol and butanol diesel blends. Fuel Process Technol 2012;100:63–72.
[7] Yao M, Wang H, Zheng Z, Yue Y. Experimental study of n-butanol additive and multi-injection on HD diesel engine performance and emissions. Fuel 2010;89(9):2191–201.
[8] Rakopoulos DC, Rakopoulos CD, Giakoumis EG, Dimaratos AM, Kyritsis DC. Effects of butanol–diesel fuel blends on the performance and emissions of a high-speed DI diesel engine. Energy Convers Manage 2010;51(10):1989–97.
[9] Zheng M, Han X, Asad U, Wang J. Investigation of butanol-fuelled HCCI combustion on a high efficiency diesel engine. Energy Convers Manage 2015;98:215–24.
[10] He B-Q, Yuan J, Liu M-B, Zhao H. Combustion and emission characteristics of a n-butanol HCCI engine. Fuel 2014;115:758–64.
[11] Maurya RK, Agarwal AK. Combustion and emission characterization of n-butanol fueled HCCI engine. J Energy Res Technol 2015;137.
[12] Warnatz J, Maas U, Dibble RW. Combustion: physical and chemical fundamentals, modeling and simulation, experiments, pollutant formation. 4th ed. Springer; 2006.
[13] Epping K, Aceves S, Bechtold R, Dec J. The potential of HCCI combustion for high efficiency and low emissions. SAE technical paper 2002-01-1923; 2002.
[14] Gray AW, Ryan TW. Homogeneous charge compression ignition (HCCI) of diesel fuel. SAE technical paper 971676; 1997.
[15] Christensen M, Johansson B, Einewall P. Homogeneous charge compression ignition (HCCI) using isooctane, ethanol and natural gas – a comparison with spark ignition operation. SAE technical paper 972874; 1997.
[16] Gnanam G, Sobiesiak A, Reader G, Zhang C. An HCCI engine fuelled with iso-octane and ethanol. SAE technical paper 2006-01-3246; 2006.
[17] Mack JH, Flowers DL, Buchholz BA, Dibble RW. The effect of the di-tertiary butyl peroxide (DTBP) additive on HCCI combustion of fuel blends of ethanol and diethyl ether. SAE technical paper 2005-01-2135; 2005.
[18] Turkcan A, Ozsezen AN, Canakci M. Experimental investigation of the effects of different injection parameters on a direct injection HCCI engine fueled with alcohol–gasoline fuel blends. Fuel Process Technol 2014;126:487–96.
[19] Santoso H, Matthews J, Cheng WK. Managing SI/HCCI dual-mode engine operation. SAE technical paper 2005-01-0162; 2005.
[20] Christensen E, Yanowitz J, Ratcliff M, McCormick RL. Renewable oxygenate blending effects on gasoline properties. Energy Fuels 2011;25:4723–33.
[21] Oakley A, Zhao H, Ladommatos N, Ma T. Experimental studies on controlled autoignition (CAI) combustion of gasoline in a 4-stroke engine. SAE technical paper 2001-01-1030; 2001.
[22] Yao M, Zheng Z, Liu H. Progress and recent trends in homogeneous charge compression ignition (HCCI) engines. Prog Energy Combust Sci 2009;35:398–437.
[23] Easley WL, Agarwal A, Lavoie GA. Modeling of HCCI combustion and emissions using detailed chemistry. SAE technical paper 2001-01-1029; 2001.
[24] Zheng Z, Yao M, Chen Z, Zhang B. Experimental study on HCCI combustion of dimethyl ether (DME)/methanol dual fuel. SAE technical paper 2004-01-2993; 2004.
[25] Zhang Y, He B-Q, Xie H, Zhao H. The combustion and emission characteristics of ethanol on a port fuel injection HCCI engine. SAE technical paper 2006-01-0631; 2006.
[26] Mack JH, Aceves SM, Dibble RW. Direct use of wet ethanol in a homogeneous charge compression ignition (HCCI) engine. Energy 2009;34(6):782–7.
[27] Maurya RK, Agarwal AK. Experimental study of combustion and emission characteristics of ethanol fuelled port injected homogeneous charge compression ignition (HCCI) combustion engine. Appl Energy 2011;88(4):1169–80.
[28] Sjöberg M, Dec J. Ethanol autoignition characteristics and HCCI performance for wide ranges of engine speed, load and boost. SAE Int J Engines 2010;3(1):84–106.
[29] Viggiano A, Magi V. A comprehensive investigation on the emissions of ethanol HCCI engines. Appl Energy 2012;93:277–87.
[30] Yang Y, Dec J, Dronniou N, Simmons B. Characteristics of isopentanol as a fuel for HCCI engines. SAE Int J Fuels Lubr 2010;3(2):725–41.
[31] Sjöberg M, Dec JE. Ethanol autoignition characteristics and HCCI performance for wide ranges of engine speed, load and boost. SAE Int J Engines 2010;3:84–106.
[32] Ebrahimi K, Shahbakhti M, Koch C. Comparison of butanol/n-heptane to PRF blended fuels in HCCI engines. In: Proceedings of combustion institute – Canadian section, spring technical meeting, University of Manitoba; 2011.
[33] Saisirirat P, Foucher F, Chanchaona S, Mounaim-Rousselle C. Effects of ethanol, n-butanol/n-heptane blended on low temperature heat release and HRR phasing in diesel-HCCI. SAE technical paper 2009-24-0094; 2009.
[34] DelVescovo D, Wang H, Wissink M, Reitz R. Isobutanol as both low reactivity and high reactivity fuels with addition of di-tert butyl peroxide (DTBP) in RCCI combustion. SAE Int J Fuels Lubr 2015;8(2):329–43.
[35] Yap D, Megaritis A. Applying forced induction to bioethanol HCCI operation with residual gas trapping. Energy Fuels 2005;19:1812–21.
[36] Sarathy SM, Vranckx S, Yasunaga K, Mehl M, Oßwald P, Metcalfe WK, et al. A comprehensive chemical kinetic combustion model for the four butanol isomers. Combust Flame 2012;159(6):2028–55.
[37] Grana R, Frassoldati A, Faravelli T, Niemann U, Ranzi E, Seiser R, et al. An experimental and kinetic modeling study of combustion of isomers of butanol. Combust Flame 2010;157(11):2137–54.
[38] Hansen N, Merchant SS, Harper MR, Green WH. The predictive capability of an automatically generated combustion chemistry mechanism: chemical structures of premixed iso-butanol flames. Combust Flame 2013;160(11):2343–51.
[39] Togbé C, Mzé-Ahmed A, Dagaut P. Kinetics of oxidation of 2-butanol and isobutanol in a jet-stirred reactor: experimental study and modeling investigation. Energy Fuels 2010;24:5244–56.
[40] Shahbakhti M, Ghazimirsaied A, Audet A, Koch C. Combustion characteristics of butanol/n-heptane blend fuels in an HCCI engine. In: Proceedings of combustion institute – Canadian section, spring technical meeting, Carleton University, Ottawa; 2010.
[41] Jin C, Yao M, Liu H, Lee C-F, Ji J. Progress in the production and application of n-butanol as a biofuel. Renew Sustain Energy Rev 2011;15(8):4080–106.
[42] Atsumi S, Hanai T, Liao JC. Non-fermentative pathways for synthesis of branched-chain higher alcohols as biofuels. Nature 2008;451:86–9.

[43] Blombach B, Riester T, Wieschalka S, Ziert C, Youn J-W, Wendisch VF, et al. Corynebacterium glutamicum tailored for efficient isobutanol production. Appl Environ Microbiol 2011;77:3300–10.
[44] Higashide W, Li Y, Yang Y, Liao JC. Metabolic engineering of Clostridium cellulolyticum for production of isobutanol from cellulose. Appl Environ Microbiol 2011;77:2727–33.
[45] Regalbuto C, Pennisi, Wigg MB, Kyritsis D. Experimental investigation of butanol isomer combustion in spark ignition engines. SAE technical paper 2012-01-1271; 2012.
[46] Mack JH, Butt RH, Chen Y, Chen JY, Dibble RW. Experimental and numerical investigation of ion signals in boosted HCCI combustion using cesium and potassium acetate additives. Energy Convers Manage 2016;108:181–9.
[47] Vuilleumier D, Selim H, Dibble RW, Sarathy M. Exploration of heat release in a homogeneous charge compression ignition engine with primary reference fuels. SAE technical paper 2013-01-2622; 2013.
[48] Savitzky A, Golay MJE. Smoothing and differentiation of data by simplified least squares procedures. Anal Chem 1964;36(July):1627–39.
[49] Woschni G. A universally applicable equation for the instantaneous heat transfer coefficient in the internal combustion engine. SAE technical paper 670931; 1967.
[50] Vibe II. Brennverlauf und Kreisprozess von Verbrennungsmotoren. VEB Verlag Technik; 1970.
[51] Eng J. Characterization of pressure waves in HCCI combustion. SAE technical paper 2002-01-2859; 2002.
[52] Heywood JB. Internal combustion engine fundamentals. McGraw-Hill series in mechanical engineering. New York: McGraw-Hill; 1988.
[53] Dernotte J, Mounaim-Rousselle C, Halter F, Seers P. Evaluation of butanol–gasoline blends in a port fuel-injection, spark-ignition engine. Oil Gas Sci Technol 2010;65(2):345–51.
[54] Sjöberg M, Dec JE. Comparing late-cycle autoignition stability for single- and two-stage ignition fuels in HCCI engines. In: Proceedings of the combustion institute, vol. 31 II; 2007. p. 2895–902.